

Thermal Shock Resistances and the Irradiation Effects of Graphites and C/C-Composites for Fusion Reactor Devices

著者	Sato Sennosuke, Kurumada Akira, Kawamata Kiyohiro, Ishida Ryohei
journal or publication title	Science reports of the Research Institutes, Tohoku University. Ser. A, Physics, chemistry and metallurgy
volume	35
number	2
page range	229-236
year	1991-03-05
URL	http://hdl.handle.net/10097/28341

Thermal Shock Resistances and the Irradiation Effects of
Graphites and C/C-Composites for Fusion Reactor Devices

Sennosuke Sato*, Akira Kurumada*, Kiyohiro Kawamata* and Ryohei Ishida**
(Received November 2 , 1990)

Synopsis

Graphites and/or C/C-composites as plasma-facing first wall components for fusion reactor devices are subjected occasionally to plasma disruption. Therefore the thermal shock resistances and fracture toughnesses of these materials must be evaluated to assure appropriate performances. In this study, the thermal shock resistance and fracture toughness of several kinds of graphites and C/C-composites for candidate first wall component tiles are evaluated. The mechanical and fracture mechanics properties for these specimens are also measured. Then, two graphites and three C/C-composites are irradiated with $1.1-1.9 \times 10^{21} \text{ n/cm}^2$ (Energy > 29 fJ) at 650-1000°C in a fission reactor (Japan Material Testing Reactor, JMTR) and the degradations in the thermal shock resistances and fracture toughnesses and the changes of mechanical and fracture mechanics properties due to the neutron irradiation are quantitatively studied.

1. Introduction

Graphites and C/C-composites as plasma-facing first wall components for fusion reactor devices are so severely subjected to plasma disruption. Therefore thermal shock resistance and fracture toughness for these materials must be evaluated to see whether or not they have appropriate performances. In this study, thermal shock resistance and fracture toughness for several kinds of graphites and C/C-composites as candidate first wall components are determined by means of arc discharge heating for disk specimens. The mechanical and fracture mechanics properties for these materials are also measured. Then, two graphites and three C/C-composites are irradiated with $1.1-1.9 \times 10^{21} \text{ n/cm}^2$ (Energy > 29 fJ) at 650-1000°C in a fission reactor (Japan Material Testing Reactor, JMTR). The degradations in thermal shock resistance and fracture toughness and the changes of mechanical and fracture mechanics properties due to neutron irradiation are quantitatively studied.

* Dep. of Mech. Eng., Faculty of Eng., Ibaraki University, Hitachi 316

** Dep. of Mech. Eng., Faculty of Eng., Univ. of Osaka Prefecture, Sakai 591

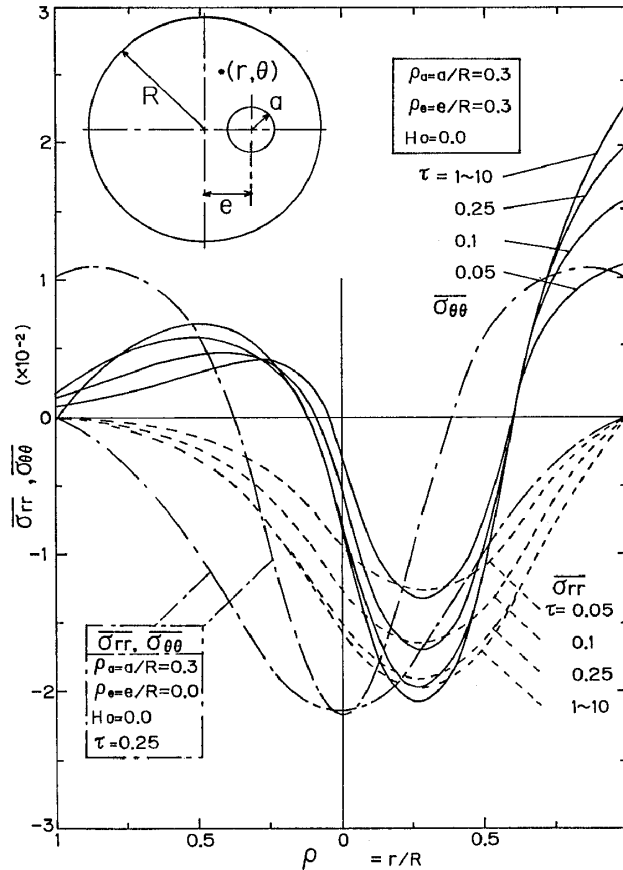


Fig. 1 Dimensionless radial and circumferential stress distributions of a disk with circular heat source area located eccentrically for various dimensionless time τ .

II. Experimental Methods

1 Thermal shock resistance and fracture toughness

Transient thermal stresses of a thin circular disk, which is locally heated at an arbitrary eccentric position, change considerably depending on the shape and the relative position of heating area.^{1,2} In this analysis, we considered the nondimensional Biot number H_0 on both surfaces of the disk. Fig.1 shows nondimensional radial and circumferential stress distributions of a disk with circular heat source area located eccentrically in various nondimensional time τ . In result, the radial stress σ_{rr} are by nature all compressive, with the maxima occurring at the center of heating area. It reduces to zero at the outer periphery of the disk. On the other hand, the circumferential stress $\sigma_{\theta\theta}$ also has the maximum compressive stress occurring at the center of heating area. However, it turns to tensile stress at the outside of heating area, and attains their maxima at the outer periphery near heating area of the disk. On the other side of the radius, the tensile stress attains the maxima once, and then decreases. The stresses saturate to almost the maximum value for nondimensional time $\tau > 0.25$. Therefore, for brittle materials such as

graphite, the primary tensile fracture due to the circumferential maximum stress $\overline{\sigma_{\theta\theta \max}}$ apt to occur at the outer periphery.

Now, when a heat quantity per unit volume and unit time Q_0 ($=\beta W/\pi a^2 h$; β is a heating efficiency, W is a heating power, a and h are a radius of a heating area and a thickness of the disk) attained a critical value, the disk is fractured. Therefore, we can evaluate thermal shock resistance $\Delta^{(3)}$ as a lumped material property, irrespective of the individual material property as follows;

$$\Delta \equiv \frac{\sigma_t k}{E \alpha} = \frac{\overline{\sigma_{\theta\theta \max}} \beta W}{\pi (a/R)^2 h} \quad (1)$$

where σ_t is tensile strength, k is thermal conductivity, E is Young's modulus, α is thermal expansivity and R is the radius of the disk.

Meanwhile, we have carried out an analysis of the stress intensity factor for the aforementioned transient thermal stress problem by using a disk having an edge slit and an eccentrically located heating area.⁽²⁾ In result, nondimensional stress intensity factor F_{I_0} ($=K_{I_0} k/\sqrt{\pi c E \alpha Q_0 R^2}$, K_{I_0} is the stress intensity factor at a crack tip due to thermal stress and c is a slit depth.) was calculated. Now, if the cracking propagates from the tip of the edge slit when a heating power of W is applied, we can evaluate thermal shock fracture toughness $\nabla^{(4)}$ as a lumped material properties, as follows;

$$\nabla \equiv \frac{K_{I_0} k}{E \alpha} = \frac{F_{I_0} \sqrt{\pi c} \beta W}{\pi (a/R)^2 h} \quad (2)$$

The value of ∇ is considered to represent the fracture toughness or the stress intensity factor at the slit tip under thermal stress corresponding to Δ .

In this study, thermal shock resistance and fracture toughness for graphites and C/C-composites were measured by utilizing the central arc discharge heating method.^(3,4) Most of the testings in this study were carried out using disk specimens of 30mm in diameter and 3mm in thickness, under the condition of the heating area ratio $\rho_a = a/R = 0.3$ or 0.5 and the slit depth ratio $\rho_c = c/R = 0.3$. The value of heating time t_* for the disk of 30mm in diameter was evaluated as 3.0 sec corresponding to nondimensional time $\tau = 0.25$.

2 Other properties

By using similar disk specimens, we also measured thermal diffusivity $\kappa^{(3)}$, diametral compressive strength $\sigma_{HC}^{(5)}$ by using circular anvils, mode I and II fracture toughnesses K_{Ic} and $K_{IIc}^{(6)}$ of the disk with a central slit. In addition, Young's modulus E by measuring ultrasonic pulse speed⁽⁷⁾, dimensional change, electric resistance, bending strength and relative Charpy impact energy after irradiation were also measured by using long circular rod specimens.

3 Graphites and C/C-composites specimens

In this study, four kinds of isostatically molded graphites of fine grain petroleum coke were used with the exception of HCB-18, which was a press molded binderless graphite of very fine grain mesophase pitch carbon. And five kinds of C/C-composites which were reinforced by felt carbon fiber, with the exception of 2D-C/C reinforced long carbon fiber cloth were used. Some specimens of C/C-composites, with the exception of PCC-1S(\perp) and -2S(\perp) corresponding to the vertical direction, were cut from the surface of the plate materials.

4 Neutron irradiation

The specimens of IG-110, HCB-18⁽⁸⁾, C/C-A, C/C-B and 2D-C/C were exposed to neutron irradiation in JMTR. The irradiation conditions are with $1.1-1.9 \times 10^{21}$ n/cm² (Energy > 29fJ) at 650-1000°C. For neutron irradiation, the smaller disks of 20mm in diameter and 2mm in thickness were used.

III. Experimental Results and Discussion

1 Thermal shock resistance and fracture toughness

Fig.2 and 3 show thermal shock resistances and thermal shock fracture toughnesses of tested graphites and C/C-composites. The lower and upper limits of the black ranges in the figures correspond to the range of scatter in the fractured specimens. Among five kinds of graphites, IG-430u and ETP-10 showed high thermal shock resistance and fracture toughness. But the values of HCB-18 were low.

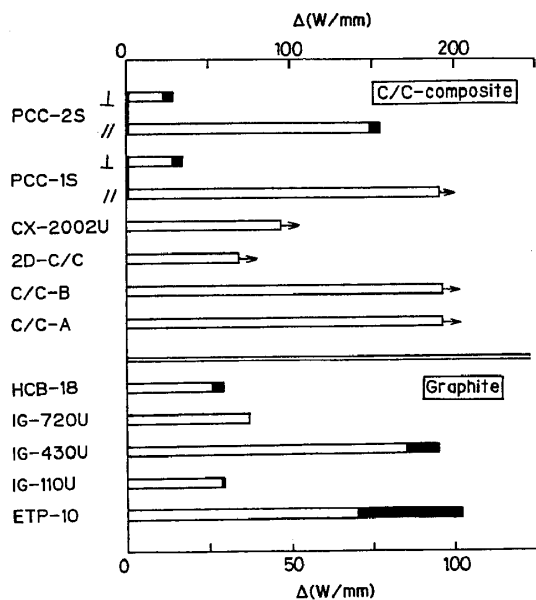


Fig. 2 Thermal shock resistances of tested graphites and C/C-composites.

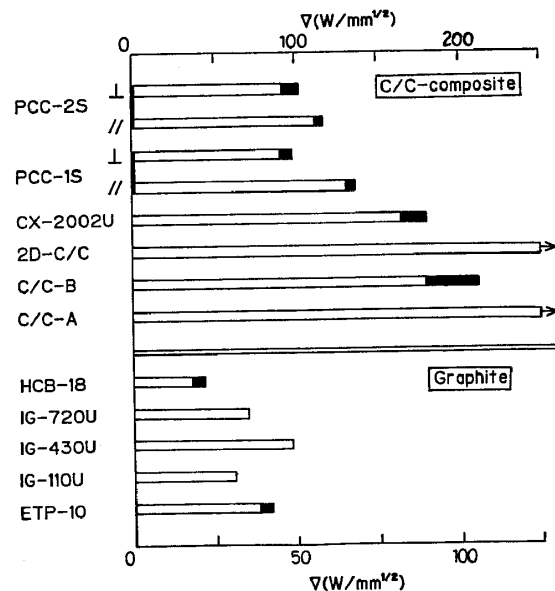
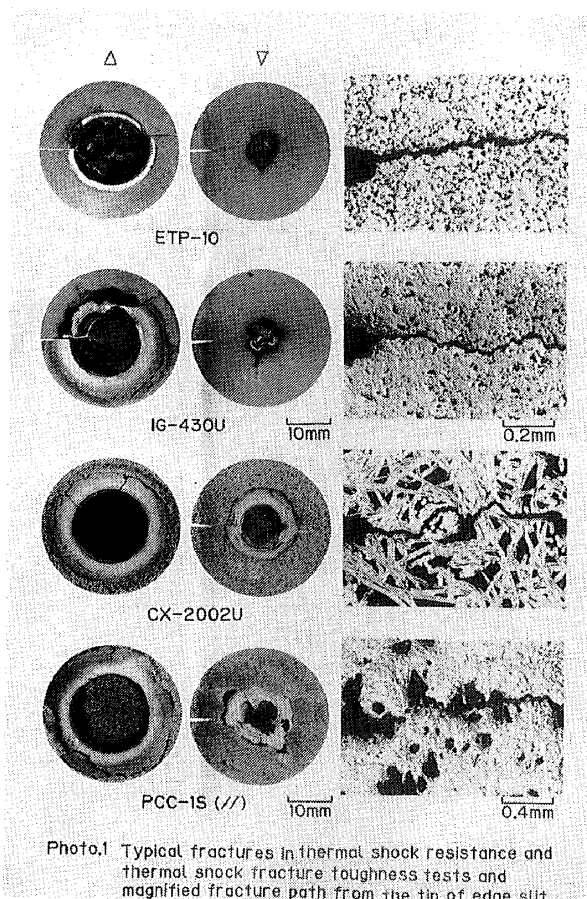


Fig. 3 Thermal shock fracture toughnesses of tested graphites and C/C-composites.



Thermal shock resistance and fracture toughness for C/C-composites are significantly higher than those of graphites. Note, however, that thermal shock resistances corresponding to the vertical direction for PCC-1S(⊥) and -2S(⊥) are considerably small. They are about the same order of magnitude as those for graphites HCB-18 and IG-110u. Photo.1 shows typical fractures in thermal shock resistance and thermal shock fracture toughness tests and magnified fracture path from the tip of edge slit of graphites and C/C-composites. Table 1(a) and (b) summarize mean values of experimental results of graphites and C/C-composites, containing other mechanical and fracture mechanics properties.

2 Neutron Irradiation Effects

Table 2 summarizes mean values of experimental results obtained for two graphites and three C/C-composites specimens before and after neutron irradiation. The numbers inside the parenthesis show the ratio of values "after" and "before" irradiation.

In the case of graphites, thermal shock resistance and fracture toughness after irradiation degraded to about 0.68-0.78 times of the values before irradiation. The degradation ratio was about the same as the mean value previously obtained for four kinds of HTGR graphites⁽²⁾. Degradation ratios of C/C-composites were not exactly determined, with the exception of thermal shock fracture toughness of C/C-B composite.

Table 1 (a) Mean values of experimental results of graphites

Material	N*	ETP-10	IG-110u	IG-430u	IG-720u	HCB-18
Bulk density γ (g/cm ³)	15	1.72	1.75	1.85	1.81	2.00
Young's modulus E (GPa)	6	10.7	9.6	10.9	10.1	13.7
Bending strength σ_b (MPa)	6	62.3	48.6	80.6	71.2	78.4
Diametral compressive strength σ_{Ht} (MPa)	5	18.0	14.9	19.4	23.0	37.1
Rockwell hardness H _{R15X}	6	81.4	74.2	83.6	87.9	91.0
Mode I fracture toughness K _{IC} (MPam ^{1/2})	5	0.89	0.82	1.04	1.01	0.75
Mode II fracture toughness K _{IIc} (MPam ^{1/2})	5	1.01	0.97	1.21	1.17	0.94
K _{IIc} /K _{IC}	10	1.13	1.18	1.16	1.16	1.25
Thermal shock resistance Δ (W/mm)	10	85.7	29.2	90.1	37.0	27.5
Thermal shock fracture toughness ∇ (W/mm ^{1/2})	9	39.7	30.7	48.5	35.3	20.0

* N means numbers of test pieces.

Table 1 (b) Mean values of experimental results of C/C-composites

Material	*	N**	C/C-A	C/C-B	2D-C/C	CX-2002u	PCC-1S	PCC-2S
Bulk density γ (g/cm ³)		15	1.58	1.77	1.74	1.68	1.89	1.85
Young's modulus E (GPa)		6	13.5	26.3	23.8	12.7	35.7	18.0
	\perp	(6)	-	-	-	-	(3.52)	(2.97)
Bending strength σ_b (MPa)		6	65.7	96.9	117	66.0	79.5	38.3
	\perp	(6)	57.4	94.5	116	-	(24.8)	(12.0)
Diametral compressive strength σ_{Ht} (MPa)			-	-	-	-	-	-
	\perp		-	-	-	-	-	-
Rockwell hardness H _{R15X}		6	42.0	44.0	74.8	54.1	-	-
	\perp		-	-	-	-	-	-
Mode I fracture toughness K _{IC} (MPam ^{1/2})		5	2.96	3.44	5.26	1.04	-	-
	\perp	(5)	2.14	3.03	-	-	-	-
Mode II fracture toughness K _{IIc} (MPam ^{1/2})		5	3.79	4.39	-	1.61	-	-
	\perp		-	-	-	-	-	-
K _{IIc} /K _{IC}		10	1.28	1.28	-	1.55	-	-
Thermal shock resistance Δ (W/mm)		10	>194	>194	>68.3	>94.5	>191	152
	\perp	(8)	-	-	-	-	30.9	25.9
Thermal shock fracture toughness ∇ (W/mm ^{1/2})		9	739	196	>856	172	135	115
	\perp	(8)	-	-	-	-	95.4	97.5

() indicates interlayer properties.

* || and \perp mean parallel and perpendicular to the molding direction.

** N means numbers of test pieces.

Table 2 Mean values of experimental results of graphites and C/C-composites before and after neutron irradiation.

Material	N.:	IG-110		HCB-18		C/C-A		C/C-B		2D-C/C	
		Before	After	Before	After	Before	After	Before	After	Before	After
Bulk density	15	1.75	1.75	2.00	2.01	1.58	1.60	1.77	1.80	1.74	1.82
γ (g/cm ³)			(1.00)		(1.01)		(1.01)		(1.02)		(1.05)
Total porosity	15	22.6	22.6	11.5	11.1	30.1	29.2	21.7	20.4	14.2	10.2
P (%)			(1.00)		(0.97)		(0.97)		(0.94)		(0.72)
Young's modulus	6	7.8	11.8	13.7	20.5	13.5	19.2	26.3	34.2	23.8	31.6
E (GPa)			(1.51)		(1.50)		(1.42)		(1.30)		(1.33)
Compressive strength	5	70.5	89.2	192.1	232.4	44.9	58.4	66.3	81.2	-	-
σ_c (MPa)			(1.27)		(1.21)		(1.30)		(1.22)		
Bending strength	6	38.7	47.6	78.4	94.4	65.7	81.5	96.9	119.2	117	145
$\sigma_b \parallel^{**}$ (MPa)			(1.23)		(1.20)		(1.24)		(1.23)		(1.24)
Bending strength	6	-	-	-	-	57.4	79.8	94.5	110.0	116	143
$\sigma_b \perp^{**}$ (MPa)							(1.39)		(1.16)		(1.23)
Diametral compressive strength σ_{Ht} (MPa)	4	15.3	18.5	37.1	44.5	-	-	-	-	-	-
			(1.21)		(1.20)						
Tensile strength	5	23.7*	27.6*	52.0*	61.4*	35.7	-	55.4	-	90.1	114
σ_t (MPa)			(1.16)		(1.18)						(1.27)
Dimensional change(%)	6	-	-0.04	-	-0.14	-	-0.34	-	-0.64	-	-1.54
Electric resistance	6	1150	1927	1208	1970	-	-	400	580	1217	2323
ρ ($\mu\Omega\text{cm}$)			(1.68)		(1.63)				(1.45)		(1.91)
Rockwell hardness	4	71	78	91	99	42	50	44	58	74.8	80.6
H _{R15X}			(1.10)		(1.09)		(1.19)		(1.32)		(1.08)
Impact absorbed energy	4	0.41	0.42	0.47	0.48	1.23	1.28	1.16	1.18	1.54	1.66
$E_c \parallel$ (J/cm ²)			(1.02)		(1.02)		(1.04)		(1.02)		(1.08)
Impact absorbed energy	4	-	-	-	-	1.22	1.28	1.13	1.16	1.54	1.67
$E_c \perp$ (J/cm ²)							(1.05)		(1.03)		(1.08)
Mode I fracture toughness	4	0.78	1.01	0.75	0.99	2.96	3.65	3.44	4.14	5.26	5.77
$K_{IC} \parallel$ (MPam ^{1/2})			(1.29)		(1.32)		(1.23)		(1.20)		(1.10)
Mode I fracture toughness	4	-	-	-	-	2.14	2.65	3.03	3.94	-	-
$K_{IC} \perp$ (MPam ^{1/2})							(1.24)		(1.30)		
Mode II fracture toughness	4	0.96	1.24	0.94	1.20	3.79	4.85	4.39	5.56	-	-
K_{IIC} (MPam ^{1/2})			(1.29)		(1.28)		(1.28)		(1.27)		
K_{IIC}/K_{IC}	8	1.23	1.23	1.25	1.21	1.28	1.33	1.28	1.30	-	-
Thermal diffusivity	4	48.5	26.0	39.3	21.7	62.4	48.5	56.6	45.3	47.9	25.2
κ (mm ² /s)			(0.54)		(0.55)		(0.78)		(0.80)		(0.53)
Thermal shock resistance	8	31.9	21.7	27.5	19.0	>194	>97	>194	>97	>68.3	>75.5
Δ (W/mm)			(0.68)		(0.69)		(-)		(-)		(-)
Thermal shock fracture toughness ∇ (W/mm ^{1/2})	7	34.4	26.8	20.0	14.3	739	>356	196	164	>856	221
			(0.78)		(0.72)		(-)		(0.84)		(-)
Equivalent crack length $C_o = \frac{1}{\pi} \left\{ \frac{K_{IC}}{\sigma_t} \right\}^2$	-	0.345	0.426	0.066	0.083	2.188	-	1.227	-	1.08	0.82
(mm)			(1.23)		(1.26)		(-)		(-)		(0.75)
Equivalent crack length $C_o' = \frac{1}{\pi} \left\{ \frac{\nabla}{\Delta} \right\}^2$	-	0.370	0.486	0.168	0.180	-	-	-	-	-	-
(mm)			(1.31)		(1.07)						

() indicates the ratio of values after and before irradiation.

* indicates the deduced tensile strength.

** \parallel and \perp mean parallel and perpendicular to the molding direction.

\therefore N means numbers of test pieces of after neutron irradiation.

IV. Conclusions

In this study, thermal shock resistances and thermal shock fracture toughnesses of disk specimens were determined for five kinds of graphites and six kinds of C/C-composites, which may be used as first wall components for fusion reactor devices. These measurements were also performed for neutron irradiated graphites and C/C-composites. The irradiation was carried out using a fission neutron reactor (JMTR). Although the energy spectrum and the neutron fluxes were low compared to those estimated to be in use ones in future fusion reactors, the results obtained in this study may give some information on the trend of irradiation damages as first wall components.

Tile-like plates of ETP-10, HCB-18 and C/C-B specimens had actually been used as first wall components in fusion reactor devices JT-60. According to preliminary observation, the tiles of HCB-18 graphite were found to be severely damaged after a number of "shots" during the operations, but no damage was found for the tiles of ETP-10 and C/C-B specimens. Especially, the tiles of C/C-B composite, which were placed at comparatively intense positions, showed conspicuous integrity. These results, therefore, are in good agreement with the experimental evaluations of this study.

References

- (1) S.Sato, R.Ishida, A.Kurumada and M.Chida, J. Faculty of Eng., Ibaraki Univ., 34, (1986), 115-120.
- (2) S.Sato, H.Awaji, R. Ishida, A.Kurumada and M.Chida, J. Faculty of Eng., Ibaraki Univ., 35, (1987), 115-122.
- (3) S.Sato, K.Sato, Y.Imamura and J.Kon, Carbon, 13, (1975), 309-316.
- (4) S.Sato, H.Awaji and H.Akuzawa, Carbon, 16, (1978), 103-109.
- (5) H.Awaji and S.Sato, J.Eng.Mater.and Tech., ASME-H, 101, (1979), 139-147.
- (6) H.Awaji and S.Sato, J.Eng.Mater.and Tech., ASME-H, 100, (1978), 175-182.
- (7) S.Sato and S.Miyazono, Carbon, 2, (1964), 103-114.
- (8) S.Sato, K.Kawamata, A.Kurumada, H.Ugachi, H.Awaji and R.Ishida, J. Nucl. Science and Tech., 24, No.7, (1987), 547-556.
- (9) S.Sato, Y.Imamura, K.Kawamata, H.Awaji and T.Oku, J. Nucl. Eng. and Design, 61, (1980), 383-398.